



1 Aerosol organic nitrogen across the global marine boundary

2 layer: distribution patterns and controlling factors

- Ningning Sun^{1,2}, Xu Yu^{2,3}, Jian Zhen Yu^{2,4*}, Bo Zhang¹, Yilan Li^{1,5}, Ye Hu¹, Zhe Li¹,
- 4 Zhenlou Chen¹, Guitao Shi^{1*}
- 5 ¹ Key Laboratory of Geographic Information Science (Ministry of Education), School
- 6 of Geographic Sciences and State Key Laboratory of Estuarine and Coastal Research,
- 7 East China Normal University, Shanghai, China
- 8 ² Division of Environment and Sustainability, Hong Kong University of Science &
- 9 Technology, Clear Water Bay, Kowloon, Hong Kong, China
- 10 ³ Jiangsu Key Laboratory of Atmospheric Environment Monitoring and Pollution
- 11 Control, Jiangsu Collaborative Innovation Center of Atmospheric Environment and
- 12 Equipment Technology, Joint International Research Laboratory of Climate and
- 13 Environment Change, School of Environmental Science and Engineering, Nanjing
- 14 University of Information Science and Technology, Nanjing, Jiangsu, China
- ⁴ Department of Chemistry, Hong Kong University of Science & Technology, Clear
- 16 Water Bay, Kowloon, Hong Kong, China
- ⁵ Department of Chemistry, State University of New York College of Environmental
- 18 Science and Forestry, Syracuse, NY, USA

19 20

20

22 *Correspondence:

- 23 Jian Zhen Yu (jian.yu@ust.hk)
- 24 Guitao Shi (gtshi@geo.ecnu.edu.cn)





Abstract

25

48

Organic nitrogen (ON) is an important yet poorly constrained component of aerosol 26 total nitrogen (TN), particularly over remote oceans. We quantified aerosol ON in 92 27 28 total suspended particulate samples collected across approximately 160° of latitude in 29 the marine atmospheric boundary layer (MABL) during Chinese Antarctic and Arctic expeditions (2019-2024), using a newly developed method that simultaneously 30 31 determines ON and inorganic nitrogen. A significant latitudinal gradient was observed, with significantly higher ON concentrations in the Northern Hemisphere (83.3±141.4 32 ng m⁻³) than in the Southern Hemisphere (15.4±12.4 ng mm⁻³). Regionally, coastal 33 East Asia recorded the highest ON levels (164.6±179.1 ng mm⁻³) but a lower ON/TN 34 ratio (21.1%), indicating strong terrestrial and anthropogenic influence. In contrast, 35 the Arctic Ocean had lower ON concentrations (19.1±19.0 ng mm⁻³) but the highest 36 ON/TN ratio (38.6%), suggesting dominant marine biogenic sources. The Southern 37 Ocean showed the lowest ON concentration (12.0±7.1 ng m⁻³) yet a relatively high 38 ON/TN ratio (27.8%), also pointing to oceanic origins. Near Antarctica, samples 39 influenced by sea-ice air masses displayed markedly elevated ON and ON/TN ratios. 40 41 These increases were strongly correlated with sea ice concentration and chlorophyll-a 42 exposure, indicating enhanced biogenic emissions from sea-ice-associated ecosystems. 43 This study offers the first direct ON measurements along a global MABL transect, 44 revealing distinct latitudinal and regional patterns, and emphasizing the combined roles of continental inputs and marine sources. It also identifies sea-ice dynamics as a 45 key factor influencing ON in Antarctic regions, providing crucial data for improving 46 47 atmospheric and climate models.





49 Key points.

- 50 1. Aerosol organic nitrogen (ON) in the global marine boundary layer was quantified
- along a transect from the Antarctic to the Arctic ($\sim 160^{\circ}$ latitude) for the first time.
- 52 2. A strong latitudinal gradient in ON was observed, revealing distinct hemispheric
- 53 and regional patterns.
- 3. Near Antarctic, ON concentrations and ON/TN ratios were distinctly elevated in
- sea-ice-influenced air masses, highlighting the role of sea-ice dynamics.

1. Introduction

- 57 Marine atmospheric boundary layer (MABL) aerosol particles contain significant
- 58 amounts of organic nitrogen (ON) and inorganic nitrogen (IN), both recognized as
- 59 major components of atmospheric particulate matter (Li et al., 2023). ON may
- account for roughly 20–80% of total reactive nitrogen deposition to the surface ocean,
- 61 implying a potentially large, yet uncertain, role in marine nitrogen cycling and climate
- 62 (Altieri et al., 2016, 2021). However, ON remains poorly constrained due to analytical
- 63 limitations (Baker et al., 2017). Previous studies focused on the water-soluble fraction
- of aerosol ON (WSON) inferred indirectly by subtraction IN from total nitrogen (TN)
- 65 (ON = TN IN), while the water-insoluble organic nitrogen (WION) fraction has
- been largely unquantified (Cornell, 1999; Mace et al., 2003). The subtraction
- approach is prone to errors and artifacts, especially when TN and IN concentrations
- are similar, leading to underestimation and large uncertainties in ON burdens and
- 69 fluxes.
- 70 Aerosol ON arises from diverse sources. Marine pathways include primary
- 71 emissions via sea spray enriched with organic matter from the sea surface microlayer
- 72 and secondary formation from marine precursors (e.g., alkylamines) reacting with
- acidic species (Facchini et al., 2008; Miyazaki et al., 2011a). Continental pathways
- 74 include long-range transport of organic emissions from fossil fuel combustion,
- 75 biomass burning, soils, and vegetation (Cape et al., 2011; Jickells et al., 2013; Luo et
- 76 al., 2018). Primary marine emissions inject large amounts of particulate matter
- 77 annually, carrying organic carbon and nitrogen from plankton, bacteria, and surface





78 films (Violaki et al., 2015a). Observations have shown that sea spray can carry 79 substantial ON and that WION can dominate ocean-influenced aerosol ON (Miyazaki et al., 2011a). 80 81 ON affects climate and biogeochemistry by supplying bioavailable nitrogen, modifying cloud condensation nuclei and ice-nucleating particle populations, and 82 contributing to aerosol light absorption. Hygroscopic ON compounds (e.g., amino 83 acids, amines, sugars) enhance water uptake and cloud condensation nuclei (CCN) 84 activity; some proteinaceous organics act as efficient ice nuclei (Alsante et al., 2024; 85 Chan et al., 2005). Marine alkylamines can form salts with sulfuric acid, promoting 86 new particle formation and growth, thereby linking ON to aerosol number and 87 radiative forcing (Almeida et al., 2013; Brean et al., 2021). Nitrogen-containing 88 chromophores (brown nitrogen) can dominate the absorptive properties of organic 89 aerosol regionally and contribute substantially to global absorption by carbonaceous 90 91 aerosol (Li et al., 2025). 92 Despite this importance, ON sources over remote oceans remain debated. Some 93 studies implicate continental transport (e.g., dust, anthropogenic emissions), whereas 94 others point to direct sea spray emissions or secondary formation from marine-derived alkylamines (Altieri et al., 2016; Lesworth et al., 2010; Zamora et al., 2011). 95 96 Correlations between ON and ocean biological proxies (e.g., chlorophyll-a) suggest in 97 situ marine production, particularly during phytoplankton blooms (Altieri et al., 2016; Dall'Osto et al., 2019). Yet open-ocean and polar regions, where sea-ice dynamics 98 may create distinct ON emissions, remain sparsely observed (Matsumoto et al., 2022). 99 100 Around Antarctica in particular, the paucity of direct ON measurements—especially of WION-limits understanding of ON sources, seasonality, and impacts on 101 102 high-latitude atmospheric chemistry. To address these gaps, we measured aerosol ON and IN using samples collected 103 104 during three Chinese Antarctic research expeditions campaigns, spanning ~160° of latitude from the Arctic to Antarctica. We employed a newly developed aerosol 105 nitrogen analyzer based on thermal evolution and chemiluminescence detection to 106 measure aerosol IN and ON simultaneously, eliminating subtraction-based method 107





biases and capturing both WSON and WION (Yu et al., 2021). This dataset enables
evaluation of hemispheric and regional patterns, assessment of controlling factors
(e.g., continental influence, marine biological activity), and explicit investigation of
sea-ice-associated processes near Antarctica. The results provide observational
constraints to improve representation of nitrogen cycling and atmosphere-ocean
interactions in climate and atmospheric chemistry models.

114 **2. Methodology**

115

2.1. Sample Collection

A total of 92 total suspended particulate (TSP) samples were collected during three 116 Chinese Antarctic research expeditions and one Arctic expedition aboard the 117 icebreaker R/V Xuelong. Sampling spanned a latitudinal range of approximately 160° 118 (86°N to 75°S), encompassing polar and mid-latitude marine regions. The Antarctic 119 120 samplings were conducted in October to November in 2019 (SP2019, 14 samples), November 2021 to March 2022 (SP2021, 23 samples), and October 2023 to April 121 122 2024 (SP2023, 15 samples), while the Arctic campaign occurred in July to September 123 in 2021 (40 samples). During the Antarctic campaigns, aerosols were collected using a high-volume air 124 125 sampler (HVAS, TISCH Environmental, USA; flow rate: 1.2 m³ min⁻¹) equipped with 126 pre-baked (500°C, 24 h) Whatman quartz filters (20.3 × 25.4 cm; Whatman Ltd., UK). For Arctic sampling, a DIGITEL DHA-80 sampler (flow rate: 500 L min⁻¹) with 14.2 127 cm diameter Whatman quartz filters were employed. Each sample represented a 128 48-hour integrated collection period, corresponding to 2-4° latitude traversed during 129 ship transits. To minimize contamination from ship emissions, a wind sector controller 130 restricted sampling to air masses within 120° of the ship's heading. Filters were 131 handled using nitrile gloves and masks to avoid potential contamination. 132 133 Post-sampling, filters were folded with the collection surface inward, wrapped in pre-cleaned aluminum foil, sealed in polyethylene bags, labeled with sampling time 134 and location, and stored at -20°C. Detailed protocols followed established 135 methodologies (Shi et al., 2021). Following expeditions, samples were transported to 136

138139

140141

142

143

144

145

146

147

148149

150

151

152

153

154

155





the laboratory under frozen conditions and maintained at -20°C until analysis. The sampling location for the Antarctic and Arctic campaigns are illustrated in Fig. 1.

120°W 90°W 60°W 30°W 60°E 90°E 120°E ΑO 60°N CEA 30°N 0° ▲ 2021 2019 SATO 2021/2022 2023/2024 30°S SO

Figure 1. TSP Aerosol sampling locations along the cruises path from Shanghai, China to Antarctica and Arctic.

2.2. Chemistry Analysis for major ions, EC and OC

Major ions were quantified through ion chromatographic analysis of water extracts of the aerosol samples. The extraction of filters in the laboratory followed protocols comparable to those described in the previous study (Shi et al., 2021). Prior to measurement, three-quarters of each filter was sectioned into small pieces using acid-cleaned Teflon-coated scissors and transferred into high-purity Milli-Q water (18.2 M Ω). The suspensions were subjected to ultrasonic treatment for 30 min, followed by continuous shaking at 120 rpm for 12 h to ensure thorough extraction of water-soluble components. The extracts were subsequently filtered through 0.22 μm polytetrafluoroethylene (PTFE) membranes prior to ion analysis. The concentrations of the main ions (NO3 $^-$, SO4 $^2-$, Na $^+$, NH4 $^+$, K $^+$, and Ca $^{2+}$) in the sample were determined by an ion chromatograph (AQ1100, RFIC, equipped with a CS12 column (2×250 mm) for cation analysis, AS11 column (2×250 mm) for anion analysis,





- 156 Thermo Scientific, USA), and the eluents of cation and anion were 18.00 mM
- 157 methylsulfonic acid (MSA) and potassium hydroxide (KOH), respectively. During
- sample analysis, the relative deviation of repeated assays (n = 5) of all ions is usually
- less than 5%. We used the following formula to calculate non-sea salt SO₄²⁻
- 160 (nssSO₄²⁻), non-sea salt Ca²⁺ (nssCa²⁺) and non-sea salt K^+ (nss K^+):

$$[nssSO_4^{2-}] = [total SO_4^{2-}] - 0.253 \times [Na^+]$$
 (1)

$$[\operatorname{nssCa}^{2+}] = [\operatorname{total} \operatorname{Ca}^{2+}] - 0.038 \times [\operatorname{Na}^{+}]$$
 (2)

$$[\operatorname{nssK}^+] = [\operatorname{total} K^+] - 0.037 \times [\operatorname{Na}^+]$$
 (3)

- where 0.252, 0.037, and 0.038 in the above expressions are the ratios of SO_4^{2-}/Na^+ (Xu
- 162 et al., 2013), Ca²⁺/Na⁺ (Anonymous, 1997), and K⁺/Na⁺ (Keene et al., 1986) in the sea
- water, respectively.
- 164 OC and EC concentrations were determined using a Thermal/Optical Carbon
- 165 Analyzer (DRI, Model 2001, Atmoslytic Inc., USA) following the IMPROVE
- 166 protocol as implemented by Wu et al., (2024). OC and EC measurements were
- 167 conducted for aerosol filters collected during the 2021 Arctic and 2019 Antarctic
- 168 cruises.

2.3. ON measurement

- 170 Aerosol ON and IN were simultaneously measured using the recently developed
- 171 Aerosol Nitrogen Analyzer system, which enables sensitive quantification directly
- 172 from filter samples without pretreatment. Detailed descriptions of the method are
- provided in Yu et al (2021). In brief, the analyzer integrates a thermal aerosol carbon
- analyzer and a chemiluminescence NO_x analyzer. Aerosol samples collected on quartz
- fiber filters were thermally evolved under a programmed 6-step temperature protocol
- 176 (150, 180, 300, 400, 500, and 800 °C) in a 1% $O_2/99\%$ He carrier gas. The evolved
- materials were catalytically oxidized to CO₂ and nitrogen oxides (NO_y), with the C
- 178 signal monitored via methanator-FID detection and the N signal recorded through
- 179 chemiluminescence after converting NO_y to NO. The C signal assists in
- differentiating IN and ON components, as ON aerosols produce both C and N signals
- while the IN fraction only yields an N signal. The programmed thermal evolution

194





- 182 facilitates separation of aerosol IN and ON due to their distinct thermal characteristics.
- 183 Quantification of IN and ON is achieved through multivariate curve resolution (MCR)
- data treatment of the C and N thermograms using USEPA PMF (version 5.0).

2.4. Backward Trajectory Analysis

- 186 To study air mass origins, air mass backward trajectories have been calculated using
- the Hybrid Single-Particle Lagrangian Integrated Trajectories (HY-SPLIT) model with
- 188 meteorological fields from the National Oceanic and Atmospheric Administration
- 189 (NOAA) air resources laboratory GDAS database. Five-day backward trajectories
- 190 were calculated in order to reveal the history of the air masses arriving at the sampling
- 191 site (Stein et al., 2015). Each trajectory originated at the vessel's real-time position
- with an arrival height of 20 m, capturing boundary layer transport while minimizing
- 193 local ship influence.

2.5. Probability Source Contribution Function analysis

- 195 Potential Source Contribution Function (PSCF) analysis was implemented to identify
- source regions of ON observed during the sampling period (Ashbaugh et al., 1985). A
- 197 higher PSCF value indicates a greater potential source contribution to the receptor site.
- 198 In our study, the PSCF domain was established within a grid cell encompassing all
- 199 backward trajectories. The cruises were discretized into 1° latitude × 1° longitude grid
- 200 cells. The PSCF value for cell ij was calculated as:

$$PSCF_{ij} = \frac{\sum m_{ij}}{\sum n_{ij}} \quad (4)$$

- where, m_{ij} = total trajectory endpoints within cell ij; n_{ij} = subset of endpoints
- 203 associated with aerosol component concentrations exceeding the 75th percentile of
- 204 cruise measurements. To mitigate uncertainty in cells with sparse trajectory density, a
- 205 latitude-dependent weighting function (W) was applied:

206
$$W = \begin{cases} 1.0 \text{ when } n_{ij} > N2 \\ 0.8 \text{ when } N1 < n_{ij} < N2 \\ 0 \text{ when } n_{ij} < N1 \end{cases}$$
 (5)

- where n_{ii} is the number of trajectories passing for each cell in the study period and
- $N1 = 60 \cdot \cos(\text{latitude})$, and $N2 = 300 \cdot \cos(\text{latitude})$. The cosine factor is used to

210

211

220

221

222223

224

225

227

228

229

230

231

232

233





account for the changing grid cell size with varying latitude.

2.6. Air-mass exposure to chlorophyll a

metric to assess the influence of marine biogenic emissions on a target region through air mass transport (Blazina et al., 2017; Choi et al., 2019). This approach is grounded in the well-established correlation between ocean surface phytoplankton biomass and marine biogenic emissions, particularly dimethyl sulfide (DMS), where Chl-a

The Air-mass Exposure to Chlorophyl a (Chl-a) index (AEC) serves as a quantitative

concentration acts as a robust proxy for phytoplankton abundance (Siegel et al., 2013).

The AEC index estimates the integrated exposure of an air mass to oceanic DMS source regions along its trajectory by accounting for both spatial distribution of Chl-a and atmospheric vertical mixing dynamics (Zhou et al., 2023).

For each trajectory point, Chl-a concentrations (Chlai) were obtained from satellite remote sensing products (Aqua-MODIS, OCI algorithm; 8-day composite, 4 km × 4 km resolution; https://oceancolor.gsfc.nasa.gov/l3/) within a 20-km radius. Trajectory endpoints over Antarctica, sea-ice-covered areas, or at pressures < 850 hPa were assigned Chl-a = 0 (Zhou et al., 2023). Points without valid Chl-a data were excluded. The AEC for a single trajectory was computed as:

226
$$AEC = \frac{\sum_{i=1}^{120} Chla_i \times e^{-(\frac{t_i}{120})}}{n}$$
 (6)

where t_i denotes time backward along the trajectory (hours), and n is the total number of valid trajectory points. The time points when the air mass passed over the continent or regions covered by sea ice were assigned a zero chlorophyll value. To ensure robustness, trajectories with n < 90 (75% of 120 h data points at hourly resolution) were discarded. For each sample, the final AEC value was derived from the arithmetic mean of all valid trajectories during the sampling period (Yan et al., 2024).

2.7. Sea ice concentration

In this study, remote sensing data are utilized to illustrate the spatiotemporal distribution of sea ice concentrations (SICs) in the Southern Ocean. The SIC of each





sample is calculated using the following formula:

$$SIC = \frac{\sum_{i=1}^{N_S} SIC_i}{N_S}$$
 (7)

- where SIC_i represents the average sea ice density at the endpoint of the specified track.
- Ns represents the total number of trajectory endpoints located on the sea ice area. Sea
- 240 ice concentration data are from the AMSR2 dataset (Version 5.4. University of
- 241 Bremen, Germany. Index of /amsr2/asi daygrid swath/s3125) (Melsheimer and
- 242 Spreen, 2019).

3. Results

- 244 Atmospheric ON concentrations exhibited significant hemispheric differences
- 245 (independent samples t-test; p < 0.001), with values in the Northern Hemisphere (NH:
- $246 \quad 83.3 \pm 141.4 \text{ ng m}^{-3}, N = 55)$ being approximately five times higher than those in the
- Southern Hemisphere (SH: 15.4 ± 12.4 ng m⁻³, N = 37). The ON/TN ratios showed
- 248 broadly similar magnitudes between hemispheres, with slightly higher in the NH
- 249 (30.4 \pm 13.6%) compared to the SH (27.9 \pm 10.6%). Samples from three Antarctic
- 250 cruises—SP2019 (mean = 19.4 ng m $^{-3}$; range: 9.5–555.6 ng m $^{-3}$), SP2021 (mean =
- 251 20.4 ng m⁻³; range: 1.3-81.3 ng m⁻³), and SP2023 (mean = 18.3 ng m⁻³; range:
- 252 1.8–457.0 ng m⁻³) showed no significant variation (one-way ANOVA; p > 0.2),
- 253 indicating that interannual variation was rather minor. A clear latitudinal gradient in
- 254 ON concentrations was observed along the Antarctic-to-Arctic transect, with peak
- values in the 20–40° N zone and a gradual decline toward both polar regions (Fig. 2a).
- 256 Based on spatial distribution patterns, the study transect can be divided into four
- 257 regions (Fig. 1): (1) the Arctic Ocean region (AO, north of ~60° N); (2) the Coastal
- 258 East Asia region (CEA, 20–60° N); (3) the Southeast Asia-Australia Tropical Ocean
- region (SATO, $\sim 20^\circ$ N-40° S); and (4) the Southern Ocean region (SO, south of \sim
- 260 40° S).
- 261 The CEA region exhibited the highest ON concentrations (mean = 164.6 ng m⁻³)
- but the lowest ON/TN ratio (mean = 21.1%). In contrast, the SO region showed the
- lowest ON concentrations (mean = 12.0 ng m^{-3} ; range: $1.78-32.3 \text{ ng m}^{-3}$) and higher
- 264 ON/TN ratios (mean = 27.8%). Notably, the AO region displayed the highest ON/TN



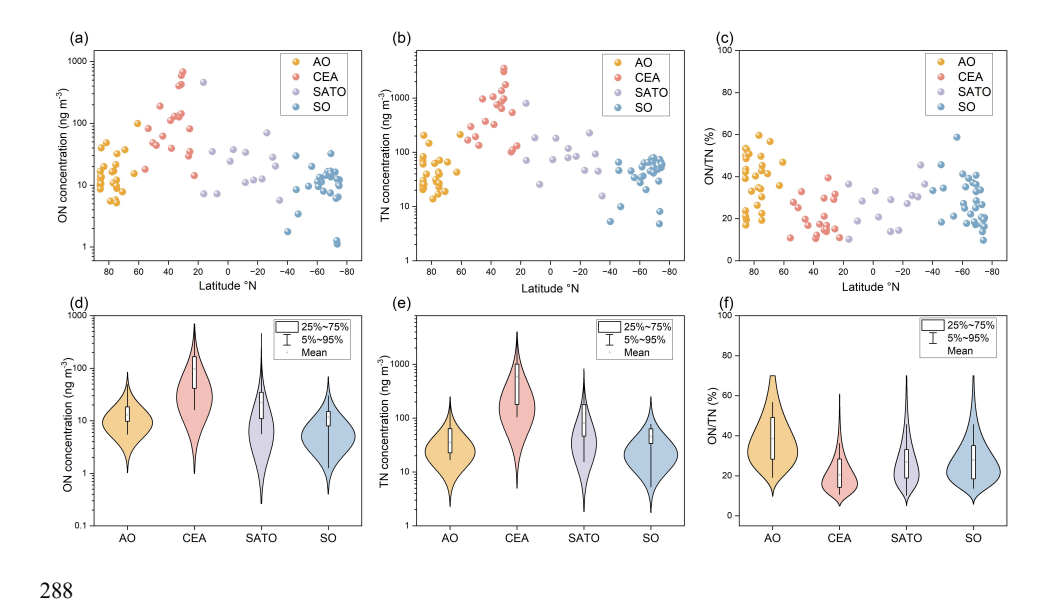


range: 5.2-32.2 ng m⁻³). The ON/TN ratio in SATO region (26.8%) is similar to that 266 of SO but with a lower ON concentration (mean = 23.4 ng m⁻³; range: 5.7–70.1 ng 267 268 m⁻³), which is much lower than the CEA region, but higher than the high latitude two pole regions. 269 Since direct measurement data of total ON in global MABL are limited, WSON 270 data were summarized for comparison (Table 1). Overall, the previous results are 271 consistent with the spatial trends of ON in our study. WSON concentrations exhibit 272 significant spatial variation, generally higher in the NH than in the SH, highlighting 273 the substantial contribution of anthropogenic sources (Violaki et al., 2015b). In 274 addition, WSON concentrations tend to be higher closer to land, while in remote 275 ocean areas, WSON levels are generally lower. The reported ratios of WSON/TN in 276 previous studies vary significantly across different investigation sites. Moreover, in 277 278 remote marine environments, the WSON/TN ratio is relatively high, suggesting that WSON plays a substantial role in the biogeochemical cycle of nitrogen within these 279 remote regions. It is important to note that most previous studies over the remote 280 281 ocean measured only WSON, without accounting for the WION. As a result, the ON/TN ratios in this region were likely underestimated. Based on our comparison, the 282 283 total ON concentration in the Southern Ocean may have been underestimated by 284 approximately 40%, hinting the significant contribution of the insoluble organic fraction that has been largely overlooked in earlier datasets due to measurement 285 method limitations. 286 287

ratios (mean = 38.6%) despite relatively low ON concentrations (mean = 19.1 ng m⁻³;







289 Figure 2. Latitudinal distributions of ON concentration, TN concentration and ON/TN ratio (a, b, 290 c), and the statistics (d, e, f) over the Arctic Ocean region (AO), the Coastal East Asia region 291 (CEA), the Southeast Asia-Australia Tropical Ocean region (SATO) and the Southern Ocean 292 region (SO), respectively.





Table 1. Measured concentrations of WSON from published reports in the marine atmospheric boundary layer.

Regions	Period	Locations	WSON (ng m ⁻³)	Ratio to TN (%)	Methods for IN	Methods for TN	Reference
Southern Atlantic	2007.01-02	35° S-45° S	119 ± 163.8	ı	IC	PO	(Violaki et al., 2015b)
the Northwest Pacific Ocean	2014.2015	25–40° N, 125–150° E	43.4–564.2	11–46	IC	PO	(Luo et al., 2018)
the coast of China the East China seas	2014.2015	$30-40^{\circ}$ N, $120-130^{\circ}$ E	96.6–7238	6-48	IC	PO	(Luo et al., 2018)
Southern Ocean	2000.11	40.41° S, 144.41° E	50.4 ± 79.8	21	IC	VV	(Mace et al., 2003)
Oahu, Hawaii	1998.7.22-8.13	21.7° N, 157.8° W	46.2	31	IC	UV	(Cornell et al., 2001)
the southern margin of the East China Sea	2005-2006	25.09° N, 121.46° E	476 ± 756	24 ± 16	IC	UV with PO	(Chen and Chen, 2010)
the western North Pacific	2008.08.24-09.13	42.98° N,144.37° E -35.65° N, 139.77° E	130 ± 61 (10–260)	67 ± 15	IC	TOC/TN analyzer	(Miyazaki et al., 2011b)
Huaniao Island	2019	30.86° N, 122.67° E	30-2810	0.13-77	IC	TOC/TN analyzer	(Tian et al., 2023)
the northern tip of Japan	2010-2012	~45.2° N, ~141.2° E	77 ± 57	12.8 ± 15.2	IC	TOC/TN analyzer	(Matsumoto et al., 2017)
the Southern Ocean	2016-2020	38.8–69.0° S, 38.1–150.8° E	4.7	20	IC	TOC/TN analyzer	(Matsumoto et al., 2022)
the Subarctic Western North Pacific Ocean	2016.7.21-8.22	30–65° N, 130–160° W	1.62–205.8	6	IC	TOC/TN analyzer	(Jung et al., 2019)
Bermuda	2011	32.27° N, 64.87° W	105 ± 191.8	50.4 ± 18.9	nutrient analyzer	TN Analyzer	(Altieri et al., 2016)

*PO: the persulfate oxidation (PO) method

*UV: ultraviolet photo-oxidation

*TN analyzer: a total organic carbon (TOC) analyzer with a TN unit

*Nutrient analyzer: automated nutrient analyzer and standard colorimetric method





4. Discussion

294

295

296

297298

299

300301

302

303

304

305

306307

308

309

310311

312

313314

315

316317

318

319

320

321322

4.1 Source identification of ON

ON in the MABL primarily originates from two main source pathways: marine emissions and long-distance continental transport. Marine sources include primary ON, predominantly associated with sea-spray particles enriched in biological material from the ocean surface microlayer, and secondary ON, which often derives from marine precursors such as alkylamines that react with acidic species to form new particles (Altieri et al., 2016; Facchini et al., 2008). Continental sources involve the long-range transport of organic emissions—including combustion byproducts, soiland vegetation-derived compounds, and biomass burning aerosols—that can significantly influence remote ocean regions (Cape et al., 2011; Jickells et al., 2013).

ON concentrations in the CEA region were the highest among all study regions, with air masses spending 22.6% of their 5-day trajectories over continental areas (Fig. 3b). A significant correlation between ON and crustal elements such as nssCa²⁺ (r = 0.75, p < 0.01; Fig. 4) likely suggests the influences of continental transport of particles on the ON levels in this region (Xiao et al., 2016). A significant correlation between ON and the anthropogenic tracer EC (r = 0.81, p < 0.01; Fig. 4) indicates that fossil fuel combustion and biomass burning are major ON sources (Shubhankar and Ambade, 2016; Wu and Yu, 2016). Similarly, the robust association between ON and $nssK^+$ (r = 0.78, p < 0.01; Fig. 4), a tracer of biomass burning, also supports contributions from agricultural and residential biomass burning (Song et al., 2018). Despite the high absolute ON concentrations, the relatively low ON/TN ratio (21.1%) likely reflects disproportionately elevated IN emissions from intensive human activities, particularly NH₃ volatilization from agriculture and vehicular NO_x emissions (Pavuluri et al., 2015). This interpretation aligns with emission inventories that identify the CEA as a global nitrogen pollution hotspot, where ON is co-emitted or formed from precursors that share common sources with EC and other combustion-related pollutants, originating from incomplete combustion and industrial processes (Deng et al., 2024).



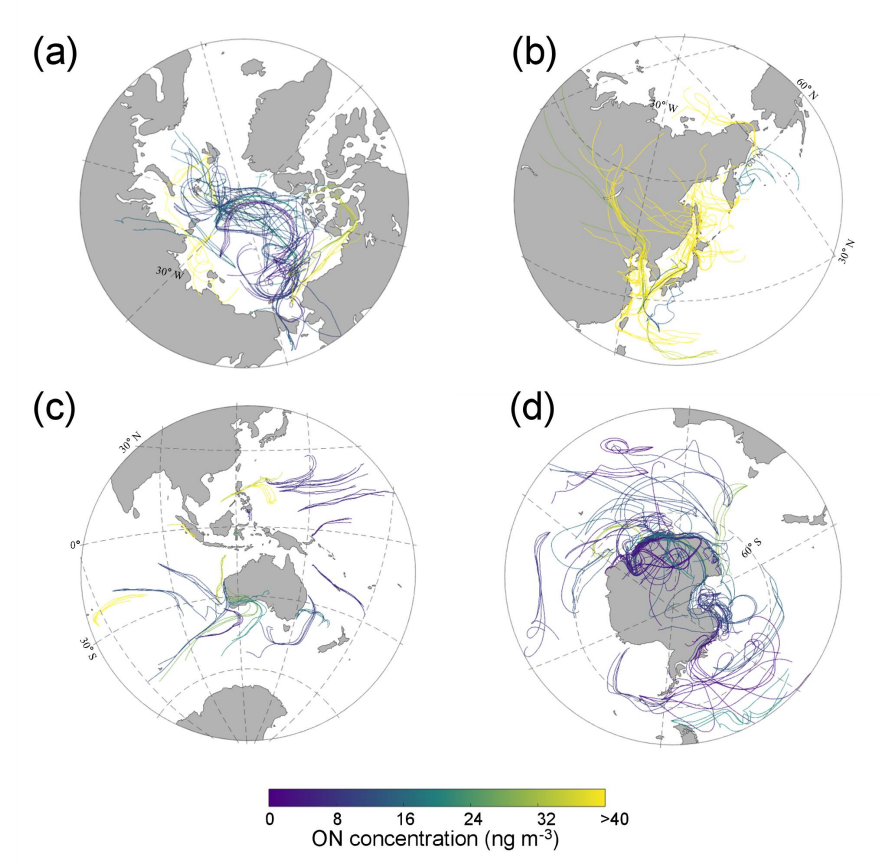


Figure 3. 5-day air-mass backward trajectories with ON concentrations and ON/TN ratios along the Chinese Arctic/Antarctic expedition voyage over the Arctic Ocean (a), the coastal East Asia (b), the Southeast Asia-Australia Tropical Ocean (c), and the Southern Ocean (d).

The SATO region exhibits intermediate level of ON concentrations (mean = 23.4 \pm 18.0 ng m⁻³), lower than those influenced by anthropogenic activities in CEA but higher than in polar regions. In this region, ON shows a significant positive correlation with nssCa²⁺ (Fig. 4; r = 0.76, p < 0.01), suggesting that continental inputs influence ON levels. In addition, backward trajectory analysis showed that samples affected by continental air masses have significantly higher ON concentrations than those exposed solely to marine air (Fig. 3c), suggesting the influences of continental sources. However, ON does not exhibit significant correlations with nssK⁺ or with EC (p > 0.05), indicating that combustion emissions may not be the primary drivers. These findings suggest that the variability of ON in the SATO region results from a mixture of marine-terrestrial interactions, primarily modulated by episodic continental





influences rather than continuous marine emissions. Notably, this region displays an elevated ON/TN ratio (Fig. 2), primarily due to its very low IN levels—approximately 85% lower than in the CEA region—which amplifies the relative contribution of ON within TN.

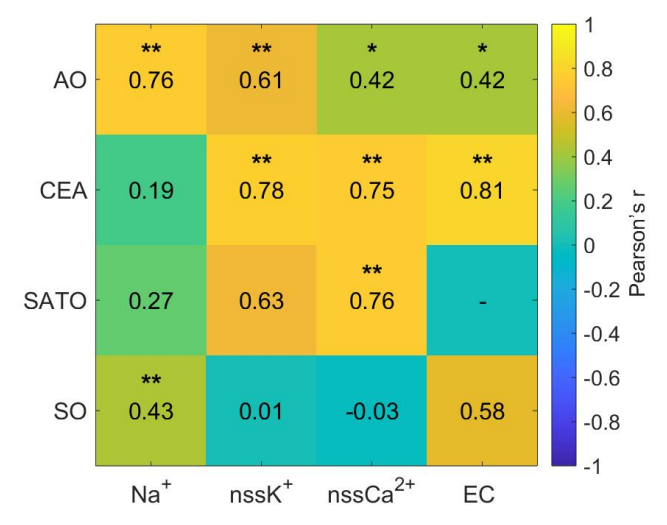


Figure 4. Spatial variations in the correlation between ON and ionic species across four regions (values in cells, with "**" indicating p < 0.01 and "*" indicating p < 0.05).

In the AO region, ON concentrations were slightly lower than in the SATO region but significantly lower than in the CEA region. In this area, ON exhibited a significant positive correlation with Na⁺, which suggest the sea salts inputs (Fig. 4; r = 0.43, p < 0.01), and also showed significant correlations with nssK⁺ (r = 0.61, p < 0.01). Its correlations with nssCa²⁺ (r = 0.42) and EC (r = 0.42) were weaker but still significant (p < 0.05). These patterns suggest that ON in the AO region may originate not only from primary sea-salt aerosols but may also be linked to biomass burning. However, the backward trajectory analysis shows no significant difference in ON concentrations between air masses influenced by continental sources and those transported solely over the ocean (Fig. S1b; independent samples t-test, p = 0.16), likely suggesting the limited role of terrestrial inputs in this region. Unlike the SATO region, where ON showed no correlation with AEC (Fig. S2b; p > 0.05), ON concentrations in the AO exhibited a strong positive correlation with the AEC (Fig. S2a; p < 0.01), suggesting that marine biological activity is a key driver of ON





variability in this region (Creamean et al., 2022). Collectively, these results demonstrate that the AO region is primarily governed by marine processes, with ON derived from both sea-spray organic enrichment and biogenic aerosol precursors, while terrestrial influences remain secondary (Nøjgaard et al., 2022).

In the SO region, ON concentrations were the lowest among all regions (mean = 12.0 ± 7.1 ng m⁻³), yet the ON/TN ratio was relatively high (27.8 \pm 11.0%). Back-trajectory analysis indicates that air masses predominantly originated from the open ocean and Antarctic continent (Fig. 3d), with minimal anthropogenic influence. ON here exhibited a significant positive correlation with Na $^+$ (Fig. 4; r = 0.43, p < 0.01), but no significant relationships with nssK⁺, nssCa²⁺ or EC. This pattern suggests that primary sea-salt emissions are a major pathway for ON in the SO atmosphere (Matsumoto et al., 2022), likely through the incorporation of marine-derived organic matter into sea-spray aerosols. Meanwhile, the absence of associations with terrestrial tracers further supports the notion that ON in this remote region is controlled primarily by natural marine processes rather than continental or anthropogenic sources (Altieri et al., 2016).

4.2 Role of sea-ice-associated biogenic processes in shaping Antarctic aerosol ON

Sea-ice and open-ocean environments create distinct conditions for the production and emission of ON. While sea ice restricts direct air—sea exchange, it hosts specialized microbial communities and accumulates organic matter within brine channels. During melt and ice-edge retreat, this organic material is released, enriching the surface microlayer and supplying precursors for aerosolization via sea spray and secondary formation (Dall'Osto et al., 2017; DeMott et al., 2016; Galgani et al., 2016; Wilson et al., 2015).

Along the Antarctic coast, we classified samples into two groups based on air-mass histories: open ocean (OO), influenced almost exclusively by open-ocean trajectories, and sea ice (SI), with air masses residing over sea ice for extended periods. SI samples exhibited significantly higher ON concentrations and ON/TN ratios than OO samples (independent-samples t-test, p < 0.01; Fig. 5a, b). Multiple lines of evidence point to sea-ice-linked biological processes as the driver of these enhancements: (1) Strong positive correlations of ON with sea-ice concentration (SIC; r = 0.86, p < 0.01) and with air-mass exposure to chlorophyll-a (AEC; r = 0.91, p < 0.01) in the SI group indicate that both ice cover and associated biological activity





elevate ON (Fig. 5c, d); (2) PSCF analysis identifies high-probability source regions (PSCF > 0.8) over sea ice and its marginal zone for SI samples (Fig. S3c), consistent with an ice-edge origin; and (3) In contrast, ON shows no significant correlation with Na⁺ (r = -0.22, p > 0.05) or with IN (p > 0.05) for SI samples (Fig. S4a,b), suggesting that primary sea-salt emissions and purely abiotic inorganic pathways are not the dominant contributors.

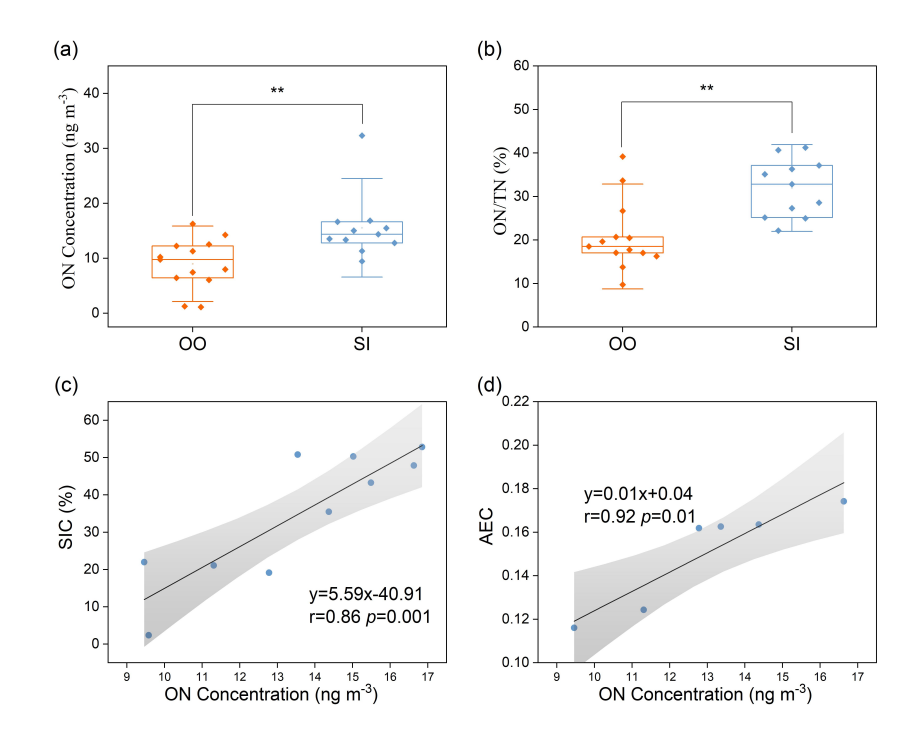


Figure 5. Comparison of measured ON concentrations (a) and ON/TN ratio (b) between SI and OO aerosol samples ("**" indicating p < 0.01). And correlations between SIC (c), AEC (d) and ON concentration in SI aerosol samples (with n = 10 and 6 for panels c and d, respectively, owing to missing satellite data and the methodologies in Sections 2.6 and 2.7).

These observations support a mechanistic pathway whereby organic matter released from sympagic (ice-associated) communities during melt enriches the surface microlayer and is transferred to the atmosphere via sea spray as ON-rich particles (DeMott et al., 2016; Wilson et al., 2015). Concurrently, a portion of this organic nitrogen is rapidly microbially degraded to volatile alkylamines (e.g., methylamines) (Taubert et al., 2017), which then form aminium salts through acid–base reactions with marine emissions-derived acids (e.g., H₂SO₄, MSA), contributing to both ON





and IN in SI conditions (Brean et al., 2021; Dawson et al., 2012; Fitzsimons et al., 2023). This process results in the formation of both organic (amine salts, contributing to ON) and inorganic nitrogen aerosol species (NH₄⁺ and NO₃⁻), which explains their elevated levels in the SI group samples (Fig. S5). The elevated ON/TN ratios in SI samples (31.0%) relative to OO samples (20.8%) further indicate a greater fractional contribution of ON under sea-ice influence (Fig. 5b), consistent with reported releases of organic material from the sympagic ecosystem during melt (Jang et al., 2023; Mirrielees et al., 2024; Yan et al., 2020).

For OO samples, PSCF hotspots (PSCF > 0.8) shift toward the offshore Southern Ocean (Fig. S3d), in line with trajectories dominated by open-ocean air masses. The positive association between ON and oceanic residence time (r = 0.66, p < 0.01; Fig. S6) suggests that, as sea-ice influence diminishes, ON variability becomes increasingly governed by open-ocean biological processes and long-range marine aerosol transport.

Overall, these results establish the ice-edge/sympagic environment as an important regulator of Antarctic aerosol ON. Sea-ice dynamics modulate both the magnitude (higher ON and ON/TN) and sources (biogenic enrichment and amine-driven secondary formation) of ON, underscoring the need to represent sea-ice-associated processes in polar atmospheric chemistry and climate models.

5. Conclusions and Implications

Taking advantage of a new analytical tool for ON and aerosol samples collected from three Antarctic and Arctic expeditions from 2019 to 2024, we quantified aerosol ON and IN in 92 TSP samples spanning 160° of latitude in the MABL. This dataset provides the first direct, subtraction-free ON measurements along a global-scale marine transect, capturing both water-soluble and water-insoluble fractions.

We observed a pronounced hemispheric and latitudinal gradient in ON, with substantially higher concentrations in the Northern Hemisphere ($83.3 \pm 141.4 \text{ ng m}^{-3}$) than in the Southern Hemisphere ($15.4 \pm 12.4 \text{ ng m}^{-3}$). Regionally, Coastal East Asia exhibited the highest ON ($164.6 \pm 179.1 \text{ ng m}^{-3}$) but a low ON/TN ratio (21.1%), consistent with strong terrestrial and anthropogenic influences that elevate IN. The Southeast Asia–Australia Tropical Ocean showed intermediate ON and a relatively high ON/TN ratio due to low IN. The Arctic Ocean had lower ON but the highest ON/TN ratio (38.6%), indicating prominent marine biogenic contributions. The





Southern Ocean showed the lowest ON (12.0 \pm 7.0 ng m⁻³) yet a relatively high 444 ON/TN ratio (27.8%), also suggestive of oceanic sources. Interannual variability 445 across the three Antarctic campaigns was minor. 446 447 Multiple lines of evidence, including correlations with tracers, back-trajectory 448 analysis, and PSCF, indicate that ON in CEA is dominated by continental inputs from combustion and dust, whereas ON in AO and SO is primarily controlled by marine 449 processes. Along the Antarctic coast, air masses influenced by sea ice exhibited 450 451 significantly higher ON and ON/TN than those influenced by the open ocean, with 452 strong positive relationships to sea-ice concentration and air-mass exposure to chlorophyll-a. These patterns point to sympagic and ice-edge biogenic 453 454 activity—through organic enrichment of sea spray and amine-driven secondary 455 formation—as key regulators of ON near Antarctica. 456 Comparison with prior WSON-only datasets suggests that earlier studies likely underestimated total ON-by approximately 40% in the Southern Ocean-due to 457 omission of WION. Accounting for both soluble and insoluble phases is therefore 458 essential for constraining nitrogen deposition to the oceans and for representing ON's 459 roles in aerosol-cloud interactions and radiative effects. 460 461 These findings fill a critical observational gap, establish robust hemispheric and regional patterns of marine aerosol ON, and provide essential constraints for 462 463 atmospheric chemistry and climate models. Future efforts should explicitly represent ON sources, including sea-ice-associated biogenic processes and amine chemistry, 464 465 and expand year-round, size-resolved, and composition-resolved measurements paired with isotopic and molecular tracers to refine source apportionment and evaluate model 466 467 parameterizations across regions and seasons. Data availability. 468 469 The data on organic nitrogen concentrations in aerosol are available at National Tibetan Plateau/Third Pole Environment Data 470 Center. DOI: 471 https://cstr.cn/18406.11.Atmos.tpdc.303043. https://doi.org/10.11888/Atmos.tpdc.303043 (Sun, 2025) [Dataset]. 472 473 Author contribution. Ningning Sun: Data curation, Writing-original draft. Yu Xu: Methodology. Bo 474 Zhang and Ye Hu: Visualization, Software. Zhe Li: Methodology. Yilan Li: Carried 475

out data analysis. Zhenlou Chen: Review. Jian Zhen Yu: Supervision, Writing -





478 Competing interests. The authors declare that they have no conflict of interest. 479 **Financial support** 480 481 This work was supported by the National Science Foundation of China (Grant Nos. 42276243 and 41922046), the Fundamental Research Funds for the Central 482 Universities, the Hong Kong Research Grants Council (1621322, 16304924 and 483 484 CRS HKUST605/24) 485 Acknowledgments The authors are grateful to CHINARE members for their support and assistance 486 487 in sampling. The authors acknowledge the availability of the Hybrid Single-Particle 488 Lagrangian Integrated Trajectory (HYSPLIT) model (available at https://www.arl.noaa.gov/hysplit/) 489

review & editing. Guitao Shi: Supervision, Writing – review & editing.





490 References

- 491 Almeida, J., Schobesberger, S., Kürten, A., Ortega, I. K., Kupiainen-Määttä, O.,
- 492 Praplan, A. P., Adamov, A., Amorim, A., Bianchi, F., Breitenlechner, M., David,
- 493 A., Dommen, J., Donahue, N. M., Downard, A., Dunne, E., Duplissy, J., Ehrhart,
- 494 S., Flagan, R. C., Franchin, A., Guida, R., Hakala, J., Hansel, A., Heinritzi, M.,
- 495 Henschel, H., Jokinen, T., Junninen, H., Kajos, M., Kangasluoma, J., Keskinen,
- 496 H., Kupc, A., Kurtén, T., Kvashin, A. N., Laaksonen, A., Lehtipalo, K.,
- Leiminger, M., Leppä, J., Loukonen, V., Makhmutov, V., Mathot, S., McGrath, M.
- J., Nieminen, T., Olenius, T., Onnela, A., Petäjä, T., Riccobono, F., Riipinen, I.,
- 499 Rissanen, M., Rondo, L., Ruuskanen, T., Santos, F. D., Sarnela, N., Schallhart, S.,
- 500 Schnitzhofer, R., Seinfeld, J. H., Simon, M., Sipilä, M., Stozhkov, Y., Stratmann,
- 501 F., Tomé, A., Tröstl, J., Tsagkogeorgas, G., Vaattovaara, P., Viisanen, Y., Virtanen,
- A., Vrtala, A., Wagner, P. E., Weingartner, E., Wex, H., Williamson, C., Wimmer,
- 503 D., Ye, P., Yli-Juuti, T., Carslaw, K. S., Kulmala, M., Curtius, J., Baltensperger,
- 504 U., Worsnop, D. R., Vehkamäki, H., and Kirkby, J.: Molecular understanding of
- sulphuric acid amine particle nucleation in the atmosphere, Nature, 502, 359 –
- 506 363, https://doi.org/10.1038/nature12663, 2013.
- Alsante, A. N., Thornton, D. C. O., and Brooks, S. D.: Effect of Aggregation and
- Molecular Size on the Ice Nucleation Efficiency of Proteins, Environ. Sci.
- Technol., 58, 4594 4605, https://doi.org/10.1021/acs.est.3c06835, 2024.
- Altieri, K. E., Fawcett, S. E., Peters, A. J., Sigman, D. M., and Hastings, M. G.:
- Marine biogenic source of atmospheric organic nitrogen in the subtropical North
- 512 Atlantic, Proc. Natl. Acad. Sci. U.S.A., 113, 925 930,
- 513 https://doi.org/10.1073/pnas.1516847113, 2016.
- 514 Altieri, K. E., Fawcett, S. E., and Hastings, M. G.: Reactive Nitrogen Cycling in the
- Atmosphere and Ocean, Annu. Rev. Earth Planet. Sci., 49, 523 550,
- 516 https://doi.org/10.1146/annurev-earth-083120-052147, 2021.
- Anonymous: A fresh look at element distribution in the North Pacific Ocean, EoS
- 518 Transactions, 78, 221 221, https://doi.org/10.1029/97EO00148, 1997.
- Ashbaugh, L. L., Malm, W. C., and Sadeh, W. Z.: A residence time probability
- 520 analysis of sulfur concentrations at grand Canyon National Park, Atmos. Environ.
- 521 (1967), 19, 1263 1270, https://doi.org/10.1016/0004-6981(85)90256-2, 1985.





- 522 Baker, A. R., Kanakidou, M., Altieri, K. E., Daskalakis, N., Okin, G. S.,
- Myriokefalitakis, S., Dentener, F., Uematsu, M., Sarin, M. M., Duce, R. A.,
- Galloway, J. N., Keene, W. C., Singh, A., Zamora, L., Lamarque, J.-F., Hsu, S.-C.,
- 525 Rohekar, S. S., and Prospero, J. M.: Observation- and model-based estimates of
- particulate dry nitrogen deposition to the oceans, Atmos. Chem. Phys., 17, 8189
- 527 8210, https://doi.org/10.5194/acp-17-8189-2017, 2017.
- 528 Blazina, T., Läderach, A., Jones, G. D., Sodemann, H., Wernli, H., Kirchner, J. W.,
- 529 and Winkel, L. H. E.: Marine Primary Productivity as a Potential Indirect Source
- of Selenium and Other Trace Elements in Atmospheric Deposition, Environ. Sci.
- Technol., 51, 108 118, https://doi.org/10.1021/acs.est.6b03063, 2017.
- 532 Brean, J., Dall' Osto, M., Simó, R., Shi, Z., Beddows, D. C. S., and Harrison, R. M.:
- Open ocean and coastal new particle formation from sulfuric acid and amines
- around the Antarctic Peninsula, Nat. Geosci., 14, 383 388,
- 535 https://doi.org/10.1038/s41561-021-00751-y, 2021.
- 536 Cape, J. N., Cornell, S. E., Jickells, T. D., and Nemitz, E.: Organic nitrogen in the
- atmosphere Where does it come from? A review of sources and methods,
- 538 Atmos. Res., 102, 30 48, https://doi.org/10.1016/j.atmosres.2011.07.009, 2011.
- 539 Chan, M. N., Choi, M. Y., Ng, N. L., and Chan, C. K.: Hygroscopicity of
- 540 Water-Soluble Organic Compounds in Atmospheric Aerosols: Amino Acids and
- Biomass Burning Derived Organic Species, Environ. Sci. Technol., 39, 1555 –
- 542 1562, https://doi.org/10.1021/es0495841, 2005.
- 543 Chen, H.-Y. and Chen, L.-D.: Occurrence of water soluble organic nitrogen in
- aerosols at a coastal area, J Atmos Chem, 65, 49 71,
- 545 https://doi.org/10.1007/s10874-010-9181-y, 2010.
- 546 Choi, J. H., Jang, E., Yoon, Y. J., Park, J. Y., Kim, T. W., Becagli, S., Caiazzo, L.,
- Cappelletti, D., Krejci, R., Eleftheriadis, K., Park, K. T., and Jang, K. S.:
- 548 Influence of Biogenic Organics on the Chemical Composition of Arctic Aerosols,
- 549 Global Biogeochemical Cy., 33, 1238 1250,
- 550 https://doi.org/10.1029/2019GB006226, 2019.
- 551 Cornell, S.: Water-soluble organic nitrogen in atmospheric aerosol: a comparison of
- 552 UV and persulfate oxidation methods, Atmos. Environ., 33, 833 840,
- 553 https://doi.org/10.1016/S1352-2310(98)00139-3, 1999.





- 554 Cornell, S., Mace, K., Coeppicus, S., Duce, R., Huebert, B., Jickells, T., and Zhuang,
- 555 L. Z.: Organic nitrogen in Hawaiian rain and aerosol, J. Geophys. Res., 106,
- 556 7973 7983, https://doi.org/10.1029/2000JD900655, 2001.
- Creamean, J. M., Barry, K., Hill, T. C. J., Hume, C., DeMott, P. J., Shupe, M. D.,
- Dahlke, S., Willmes, S., Schmale, J., Beck, I., Hoppe, C. J. M., Fong, A.,
- Chamberlain, E., Bowman, J., Scharien, R., and Persson, O.: Annual cycle
- observations of aerosols capable of ice formation in central Arctic clouds, Nat
- 561 Commun, 13, 3537, https://doi.org/10.1038/s41467-022-31182-x, 2022.
- Dall'Osto, M., Ovadnevaite, J., Paglione, M., Beddows, D. C. S., Ceburnis, D., Cree,
- 563 C., Cortés, P., Zamanillo, M., Nunes, S. O., Pérez, G. L., Ortega-Retuerta, E.,
- Emelianov, M., Vaqué, D., Marrasé, C., Estrada, M., Sala, M. M., Vidal, M.,
- 565 Fitzsimons, M. F., Beale, R., Airs, R., Rinaldi, M., Decesari, S., Cristina Facchini,
- M., Harrison, R. M., O' Dowd, C., and Simó, R.: Antarctic sea ice region as a
- source of biogenic organic nitrogen in aerosols, Sci Rep, 7, 6047,
- 568 https://doi.org/10.1038/s41598-017-06188-x, 2017.
- 569 Dall'Osto, M., Airs, R. L., Beale, R., Cree, C., Fitzsimons, M. F., Beddows, D.,
- Harrison, R. M., Ceburnis, D., O'Dowd, C., Rinaldi, M., Paglione, M., Nenes, A.,
- 571 Decesari, S., and Simó, R.: Simultaneous Detection of Alkylamines in the
- 572 Surface Ocean and Atmosphere of the Antarctic Sympagic Environment, ACS
- 573 Earth Space Chem., 3, 854 862,
- https://doi.org/10.1021/acsearthspacechem.9b00028, 2019.
- Dawson, M. L., Varner, M. E., Perraud, V., Ezell, M. J., Gerber, R. B., and
- Finlayson-Pitts, B. J.: Simplified mechanism for new particle formation from
- methanesulfonic acid, amines, and water via experiments and ab initio
- 578 calculations, Proc. Natl. Acad. Sci. U.S.A., 109, 18719 18724,
- 579 https://doi.org/10.1073/pnas.1211878109, 2012.
- 580 DeMott, P. J., Hill, T. C. J., McCluskey, C. S., Prather, K. A., Collins, D. B., Sullivan,
- R. C., Ruppel, M. J., Mason, R. H., Irish, V. E., Lee, T., Hwang, C. Y., Rhee, T.
- 582 S., Snider, J. R., McMeeking, G. R., Dhaniyala, S., Lewis, E. R., Wentzell, J. J.
- B., Abbatt, J., Lee, C., Sultana, C. M., Ault, A. P., Axson, J. L., Diaz Martinez,
- 584 M., Venero, I., Santos-Figueroa, G., Stokes, M. D., Deane, G. B., Mayol-Bracero,
- O. L., Grassian, V. H., Bertram, T. H., Bertram, A. K., Moffett, B. F., and Franc,
- 586 G. D.: Sea spray aerosol as a unique source of ice nucleating particles, Proc. Natl.





- 587 Acad. Sci. U.S.A., 113, 5797 5803, https://doi.org/10.1073/pnas.1514034112,
- 588 2016.
- Deng, O., Wang, S., Ran, J., Huang, S., Zhang, X., Duan, J., Zhang, L., Xia, Y., Reis,
- 590 S., Xu, J., Xu, J., De Vries, W., Sutton, M. A., and Gu, B.: Managing urban
- development could halve nitrogen pollution in China, Nat Commun, 15, 401,
- 592 https://doi.org/10.1038/s41467-023-44685-y, 2024.
- 593 Facchini, M. C., Decesari, S., Rinaldi, M., Carbone, C., Finessi, E., Mircea, M., Fuzzi,
- 594 S., Moretti, F., Tagliavini, E., Ceburnis, D., and O' Dowd, C. D.: Important
- 595 Source of Marine Secondary Organic Aerosol from Biogenic Amines, Environ.
- 596 Sci. Technol., 42, 9116 9121, https://doi.org/10.1021/es8018385, 2008.
- 597 Fitzsimons, M. F., Tilley, M., and Cree, C. H. L.: The determination of volatile amines
- in aquatic marine systems: A review, Anal. Chim. Acta, 1241, 340707,
- 599 https://doi.org/10.1016/j.aca.2022.340707, 2023.
- 600 Galgani, L., Piontek, J., and Engel, A.: Biopolymers form a gelatinous microlayer at
- the air-sea interface when Arctic sea ice melts, Sci Rep, 6, 29465,
- 602 https://doi.org/10.1038/srep29465, 2016.
- 603 Jang, J., Park, J., Park, J., Yoon, Y. J., Dall' Osto, M., Park, K.-T., Jang, E., Lee, J. Y.,
- 604 Cho, K. H., and Lee, B. Y.: Ocean-atmosphere interactions: Different organic
- 605 components across Pacific and Southern Oceans, Sci. Total Environ., 878,
- 606 162969, https://doi.org/10.1016/j.scitotenv.2023.162969, 2023.
- 607 Jickells, T., Baker, A. R., Cape, J. N., Cornell, S. E., and Nemitz, E.: The cycling of
- organic nitrogen through the atmosphere, Phil. Trans. R. Soc. B, 368, 20130115,
- 609 https://doi.org/10.1098/rstb.2013.0115, 2013.
- 610 Jung, J., Han, B., Rodriguez, B., Miyazaki, Y., Chung, H. Y., Kim, K., Choi, J.-O.,
- Park, K., Kim, I.-N., Kim, S., Yang, E. J., and Kang, S.-H.: Atmospheric Dry
- 612 Deposition of Water-Soluble Nitrogen to the Subarctic Western North Pacific
- Ocean during Summer, Atmosphere, 10, 351,
- https://doi.org/10.3390/atmos10070351, 2019.
- Keene, W. C., Pszenny, A. A. P., Galloway, J. N., and Hawley, M. E.: Sea salt
- corrections and interpretation of constituent ratios in marine precipitation, J.
- Geophys. Res., 91, 6647 6658, https://doi.org/10.1029/JD091iD06p06647,
- 618 1986.
- 619 Lesworth, T., Baker, A. R., and Jickells, T.: Aerosol organic nitrogen over the remote





- 620 Atlantic Ocean, Atmos. Environ., 44, 1887 1893,
- 621 https://doi.org/10.1016/j.atmosenv.2010.02.021, 2010.
- 622 Li, Y., Fu, T.-M., Yu, J. Z., Yu, X., Chen, Q., Miao, R., Zhou, Y., Zhang, A., Ye, J.,
- Yang, X., Tao, S., Liu, H., and Yao, W.: Dissecting the contributions of organic
- 624 nitrogen aerosols to global atmospheric nitrogen deposition and implications for
- ecosystems, Natl. Sci. Rev., 10, nwad244, https://doi.org/10.1093/nsr/nwad244,
- 626 2023.
- 627 Li, Y., Fu, T.-M., Yu, J. Z., Zhang, A., Yu, X., Ye, J., Zhu, L., Shen, H., Wang, C.,
- 4628 Yang, X., Tao, S., Chen, Q., Li, Y., Li, L., Che, H., and Heald, C. L.: Nitrogen
- dominates global atmospheric organic aerosol absorption, Science, 387, 989 –
- 630 995, https://doi.org/10.1126/science.adr4473, 2025.
- 631 Luo, L., Kao, S.-J., Bao, H., Xiao, H., Xiao, H., Yao, X., Gao, H., Li, J., and Lu, Y.:
- 632 Sources of reactive nitrogen in marine aerosol over the Northwest Pacific Ocean
- 633 in spring, Atmos. Chem. Phys., 18, 6207 6222,
- https://doi.org/10.5194/acp-18-6207-2018, 2018.
- 635 Mace, K. A., Duce, R. A., and Tindale, N. W.: Organic nitrogen in rain and aerosol at
- Cape Grim, Tasmania, Australia, J. Geophys. Res., 108, 2002JD003051,
- 637 https://doi.org/10.1029/2002JD003051, 2003.
- 638 Matsumoto, K., Yamamoto, Y., Nishizawa, K., Kaneyasu, N., Irino, T., and
- Yoshikawa-Inoue, H.: Origin of the water-soluble organic nitrogen in the
- maritime aerosol, Atmos. Environ., 167, 97 103,
- https://doi.org/10.1016/j.atmosenv.2017.07.050, 2017.
- Matsumoto, K., Kobayashi, H., Hara, K., Ishino, S., and Hayashi, M.: Water-soluble
- organic nitrogen in fine aerosols over the Southern Ocean, Atmos. Environ., 287,
- 644 119287, https://doi.org/10.1016/j.atmosenv.2022.119287, 2022.
- 645 Mirrielees, J. A., Kirpes, R. M., Costa, E. J., Porter, G. C. E., Murray, B. J., Lata, N.
- N., Boschi, V., China, S., Grannas, A. M., Ault, A. P., Matrai, P. A., and Pratt, K.
- A.: Marine aerosol generation experiments in the High Arctic during
- summertime, Elem Sci Anth, 12, 00134,
- https://doi.org/10.1525/elementa.2023.00134, 2024.
- 650 Miyazaki, Y., Kawamura, K., Jung, J., Furutani, H., and Uematsu, M.: Latitudinal
- distributions of organic nitrogen and organic carbon in marine aerosols over the
- western North Pacific, Atmos. Chem. Phys., 11, 3037 3049,

685





https://doi.org/10.5194/acp-11-3037-2011, 2011a. 653 Miyazaki, Y., Kawamura, K., Jung, J., Furutani, H., and Uematsu, M.: Latitudinal 654 distributions of organic nitrogen and organic carbon in marine aerosols over the 655 western North Pacific, Atmos. Chem. Phys., 11, 3037 - 3049, 656 https://doi.org/10.5194/acp-11-3037-2011, 2011b. 657 Nøjgaard, J. K., Peker, L., Pernov, J. B., Johnson, M. S., Bossi, R., Massling, A., 658 Lange, R., Nielsen, I. E., Prevot, A. S. H., Eriksson, A. C., Canonaco, F., and 659 660 Skov, H.: A local marine source of atmospheric particles in the High Arctic, Atmos. Environ., 285, 119241, https://doi.org/10.1016/j.atmosenv.2022.119241, 661 662 2022. Pavuluri, C. M., Kawamura, K., and Fu, P. Q.: Atmospheric chemistry of nitrogenous 663 664 aerosols in northeastern Asia: biological sources and secondary formation, Atmos. Chem. Phys., 15, 9883 - 9896, https://doi.org/10.5194/acp-15-9883-2015, 2015. 665 Shi, G., Ma, H., Zhu, Z., Hu, Z., Chen, Z., Jiang, S., An, C., Yu, J., Ma, T., Li, Y., Sun, 666 667 B., and Hastings, M. G.: Using stable isotopes to distinguish atmospheric nitrate production and its contribution to the surface ocean across hemispheres, Earth 668 Planet. Sci. Lett., 564, 116914, https://doi.org/10.1016/j.epsl.2021.116914, 2021. 669 670 Shubhankar, B. and Ambade, B.: Chemical characterization of carbonaceous carbon 671 from industrial and semi urban site of eastern India, SpringerPlus, 5, 837, 672 https://doi.org/10.1186/s40064-016-2506-9, 2016. Siegel, D. A., Behrenfeld, M. J., Maritorena, S., McClain, C. R., Antoine, D., Bailey, 673 S. W., Bontempi, P. S., Boss, E. S., Dierssen, H. M., Doney, S. C., Eplee, R. E., 674 675 Evans, R. H., Feldman, G. C., Fields, E., Franz, B. A., Kuring, N. A., Mengelt, C., 676 Nelson, N. B., Patt, F. S., Robinson, W. D., Sarmiento, J. L., Swan, C. M., Werdell, P. J., Westberry, T. K., Wilding, J. G., and Yoder, J. A.: Regional to 677 678 global assessments of phytoplankton dynamics from the SeaWiFS mission, Remote Sens. Environ., 135, 77 - 91, https://doi.org/10.1016/j.rse.2013.03.025, 679 2013. 680 681 Song, J., Zhao, Y., Zhang, Y., Fu, P., Zheng, L., Yuan, Q., Wang, S., Huang, X., Xu, W., Cao, Z., Gromov, S., and Lai, S.: Influence of biomass burning on atmospheric 682 683 aerosols over the western South China Sea: Insights from ions, carbonaceous

fractions and stable carbon isotope ratios, Environ. Pollut., 242, 1800 - 1809,

https://doi.org/10.1016/j.envpol.2018.07.088, 2018.





- 686 Stein, A. F., Draxler, R. R., Rolph, G. D., Stunder, B. J. B., Cohen, M. D., and Ngan,
- 687 F.: NOAA's HYSPLIT Atmospheric Transport and Dispersion Modeling System,
- 688 Bull. Am. Meteorol. Soc., 96, 2059 2077,
- https://doi.org/10.1175/BAMS-D-14-00110.1, 2015.
- 690 Sun, N.: Spatial distribution of organic nitrogen in the global marine boundary layer
- from Arctic to Antarctic, National Tibetan Plateau / Third Pole Environment Data
- 692 Center), https://doi.org/10.11888/Atmos.tpdc.303043, 2025.
- 693 Taubert, M., Grob, C., Howat, A. M., Burns, O. J., Pratscher, J., Jehmlich, N., Von
- Bergen, M., Richnow, H. H., Chen, Y., and Murrell, J. C.: Methylamine as a
- 695 nitrogen source for microorganisms from a coastal marine environment, Environ.
- 696 Microbiol., 19, 2246 2257, https://doi.org/10.1111/1462-2920.13709, 2017.
- 697 Tian, M., Li, H., Wang, G., Fu, M., Qin, X., Lu, D., Liu, C., Zhu, Y., Luo, X., Deng,
- 698 C., Abdullaev, S. F., and Huang, K.: Seasonal source identification and formation
- 699 processes of marine particulate water soluble organic nitrogen over an offshore
- island in the East China Sea, Sci. Total Environ., 863, 160895,
- 701 https://doi.org/10.1016/j.scitotenv.2022.160895, 2023.
- 702 Violaki, K., Sciare, J., Williams, J., Baker, A. R., Martino, M., and Mihalopoulos, N.:
- 703 Atmospheric water-soluble organic nitrogen (WSON) over marine environments:
- a global perspective, Biogeosciences, 12, 3131 3140,
- 705 https://doi.org/10.5194/bg-12-3131-2015, 2015a.
- 706 Violaki, K., Sciare, J., Williams, J., Baker, A. R., Martino, M., and Mihalopoulos, N.:
- 707 Atmospheric water-soluble organic nitrogen (WSON) over marine environments:
- a global perspective, Biogeosciences, 12, 3131 3140,
- 709 https://doi.org/10.5194/bg-12-3131-2015, 2015b.
- 710 Wilson, T. W., Ladino, L. A., Alpert, P. A., Breckels, M. N., Brooks, I. M., Browse, J.,
- 711 Burrows, S. M., Carslaw, K. S., Huffman, J. A., Judd, C., Kilthau, W. P., Mason,
- 712 R. H., McFiggans, G., Miller, L. A., Nájera, J. J., Polishchuk, E., Rae, S., Schiller,
- 713 C. L., Si, M., Temprado, J. V., Whale, T. F., Wong, J. P. S., Wurl, O.,
- 714 Yakobi-Hancock, J. D., Abbatt, J. P. D., Aller, J. Y., Bertram, A. K., Knopf, D. A.,
- and Murray, B. J.: A marine biogenic source of atmospheric ice-nucleating
- 716 particles, Nature, 525, 234 238, https://doi.org/10.1038/nature14986, 2015.
- 717 Wu, C. and Yu, J. Z.: Determination of primary combustion source organic
- carbon-to-elemental carbon (OC / EC) ratio using ambient OC and EC





- 719 measurements: secondary OC-EC correlation minimization method, Atmos.
- 720 Chem. Phys., 16, 5453 5465, https://doi.org/10.5194/acp-16-5453-2016, 2016.
- 721 Wu, G., Hu, Y., Gong, C., Wang, D., Zhang, F., Herath, I. K., Chen, Z., and Shi, G.:
- 722 Spatial distribution, sources, and direct radiative effect of carbonaceous aerosol
- along a transect from the Arctic Ocean to Antarctica, Sci. Total Environ., 916,
- 724 170136, https://doi.org/10.1016/j.scitotenv.2024.170136, 2024.
- 725 Xiao, H., Xiao, H., Luo, L., Shen, C., Long, A., Chen, L., Long, Z., and Li, D.:
- 726 Atmospheric aerosol compositions over the South China Sea:
- 727 Temporalvariability and source apportionment,
- 728 https://doi.org/10.5194/acp-2016-885, 7 November 2016.
- 729 Xu, G., Gao, Y., Lin, Q., Li, W., and Chen, L.: Characteristics of water-soluble
- 730 inorganic and organic ions in aerosols over the Southern Ocean and coastal East
- 731 Antarctica during austral summer: AEROSOL IN SOUTHERN OCEAN AND
- 732 ANTARCTICA, J. Geophys. Res. Atmos., 118, 13,303-13,318,
- 733 https://doi.org/10.1002/2013JD019496, 2013.
- Yan, J., Jung, J., Lin, Q., Zhang, M., Xu, S., and Zhao, S.: Effect of sea ice retreat on
- 735 marine aerosol emissions in the Southern Ocean, Antarctica, Sci. Total Environ.,
- 736 745, 140773, https://doi.org/10.1016/j.scitotenv.2020.140773, 2020.
- 737 Yan, S., Xu, G., Zhang, H., Wang, J., Xu, F., Gao, X., Zhang, J., Wu, J., and Yang, G.:
- 738 Factors Controlling DMS Emission and Atmospheric Sulfate Aerosols in the
- Western Pacific Continental Sea, JGR Oceans, 129, e2024JC020886,
- 740 https://doi.org/10.1029/2024JC020886, 2024.
- 741 Yu, X., Li, Q., Ge, Y., Li, Y., Liao, K., Huang, X. H., Li, J., and Yu, J. Z.:
- 742 Simultaneous Determination of Aerosol Inorganic and Organic Nitrogen by
- 743 Thermal Evolution and Chemiluminescence Detection, Environ. Sci. Technol.,
- 744 55, 11579 11589, https://doi.org/10.1021/acs.est.1c04876, 2021.
- 745 Zamora, L. M., Prospero, J. M., and Hansell, D. A.: Organic nitrogen in aerosols and
- 746 precipitation at Barbados and Miami: Implications regarding sources, transport
- and deposition to the western subtropical North Atlantic, J. Geophys. Res., 116,
- 748 D20309, https://doi.org/10.1029/2011JD015660, 2011.
- 749 Zhou, S., Chen, Y., Wang, F., Bao, Y., Ding, X., and Xu, Z.: Assessing the Intensity of
- 750 Marine Biogenic Influence on the Lower Atmosphere: An Insight into the
- 751 Distribution of Marine Biogenic Aerosols over the Eastern China Seas, Environ.

https://doi.org/10.5194/egusphere-2025-5458 Preprint. Discussion started: 28 November 2025 © Author(s) 2025. CC BY 4.0 License.





752 Sci. Technol., 57, 12741 - 12751, https://doi.org/10.1021/acs.est.3c04382, 2023.